Fourier Transform Infrared Study of the Cation Radical of P680 in the Photosystem II Reaction Center: Evidence for Charge Delocalization on the Chlorophyll Dimer†

Takumi Noguchi,* Tatsuya Tomo, and Yorinao Inoue

Photosynthesis Research Laboratory, The Institute of Physical and Chemical Research (RIKEN), Wako, Saitama 351-0198, Japan

Received June 1, 1998; Revised Manuscript Received July 20, 1998

ABSTRACT: A Fourier transform infrared (FTIR) difference spectrum of the primary electron donor (P680) of photosystem II upon its photooxidation ($P680^+$/P680) was obtained in the frequency region of 1000−3000 cm^{-1}. The reaction center (RC) complex (D1−D2−Cyt*b*559) was used for the measurements in the presence of ferricyanide as an exogenous electron acceptor. Control measurements of electronic absorption (300−1200 nm) showed that illumination of the RC complex at 150 K induced major oxidation of P680 concomitant with oxidation of a carotenoid and an accessory chlorophyll (Chl). Illumination at 250 K also specifically bleached one of the two β-carotene molecules bound to the RC complex, and the sample thus treated exhibited little formation of a carotenoid cation on subsequent illumination at 150 K. The $P680^+$/P680 FTIR difference spectrum (with minor contamination of Chl^+/Chl) was measured at 150 K using this partially carotenoid-deficient RC complex. The spectrum showed a broad positive band centered at ∼1940 cm^{-1}, which could be ascribed to an infrared electronic transition of $P680^+$ analogous to that previously observed in various bacterial P^+. This finding indicates that a positive charge is delocalized over (or hopping between) the two Chl molecules in $P680^+$. The low intensity of this electronic band compared with that of the bacterial band could have three possible explanations: weak resonance interaction between the constituent Chl molecules, an asymmetric structure of $P680^+$, and the difference in Chl species. Bands in the C═O stretching region (1600−1750 cm^{-1}) were interpreted in comparison with resonance Raman spectra of the RC complex. The negative peaks at 1704 and 1679 cm^{-1} were proposed as candidates for the keto C_9═O bands of P680. The observation that neither of these bands agreed with the main keto C_9═O band at 1669 cm^{-1} in the previous ^{3}P680/P680 FTIR spectrum [Noguchi et al. (1993) *Biochemistry 32*, 7186−7195] led to the idea that the triplet state migrates to a Chl (designated as Chl_T) different from P680 at low temperatures. Based on these results, structural models of Chl molecules including P680 and Chl_T and their coupling in the cation, triplet, and Qy singlet states are discussed.

In the photosynthetic apparatus, solar light collected by antenna pigments is transferred as excitation energy to the primary electron donor (P), which consists of (bacterio)-chlorophyll [(B)Chl][1] molecules attached on the reaction center (RC) protein. The excited singlet state of P then leads to charge separation to reduce the primary electron acceptor [pheophytin (Pheo)- or Chl-type pigment], and the electron further migrates to quinone molecules or iron−sulfur clusters across the membrane. The produced membrane potential is utilized to synthesize ATP, which is then used together with NAD(P)H, reducing power, for carbon fixation.

The RC protein of photosystem II (PS II) in plants and cyanobacteria is considered to have evolved from that of purple bacteria. The amino acid sequences of the D1 and D2 subunits of PS II are homologous to those of the L and M subunits, respectively, of purple bacteria, and the acceptor-side reaction, i.e., electron transfer from Pheo (BPheo in bacteria) to Q_A and then to Q_B, is basically identical (*1, 2*). On the electron donor side, however, a dramatic change occurred in the evolutional process from bacterial RC to PS II: PS II can oxidize water to produce O_2 and protons. Acquisition of this ability to utilize water as a terminal electron donor was a key step for photosynthetic organisms to thrive on the earth, and, furthermore, production of O_2 led the ancient atmosphere to the aerobic condition, which stimulated evolution of respiratory organisms. Although invention of the O_2-evolving Mn-cluster was no doubt the biggest event in this evolutional process of PS II, another important change was also indispensable: since water is

† This research was supported by Grants for Photosynthetic Sciences, Structural Biology Research, and Biodesign Research Program at The Institute of Physical and Chemical Research (RIKEN) given by the Science and Technology Agency (STA) of Japan. T.T. was supported by Grants for Special Postdoctoral Research and President's Special Research from The Institute of Physical and Chemical Research (RIKEN).

* Corresponding author. E-mail: tnoguchi@postman.riken.go.jp.

[1] Abbreviations: BChl, bacteriochlorophyll; BPheo, bacteriopheophytin; Chl, chlorophyll; Chl_Z, accessory chlorophyll as a peripheral electron donor of photosystem II; Cyt, cytochrome; EPR, electron paramagnetic resonance; FTIR, Fourier transform infrared; Hepes, *N*-(2-hydroxyethyl)piperazine-*N*′-2-ethanesulfonic acid; IR, infrared; Mes, 2-(*N*-morpholino)ethanesulfonic acid; P680, primary electron donor of photosystem II; Pheo, pheophytin; PS, photosystem; RC, reaction center; RR, resonance Raman.

S0006-2960(98)01297-5 CCC: $15.00
Published on Web 09/09/1998

oxidized by $P680^+$ via a tyrosine residue, Y_Z, P680 should have a redox potential higher than that of water, ~+0.8 V (*3*). In fact, the redox potential of P680 has been estimated to be ~+1.1 V (*4*), whereas that of P870 of purple bacteria is ~+0.5 V (*5*). Since simple replacement of BChl with Chl is expected to give an increase in the potential of only 0.1−0.2 V (*6*), some special change must have occurred in P680 to gain the additional potential of 0.4−0.5 V.

To clarify the mechanism of how P680 acquired such a high redox potential, it is essential to investigate the structure of P680 and its interaction with surrounding proteins. So far, some characteristics of P680 distinct from bacterial P870 have been reported; while P870 has a dimeric BChl structure with strong coupling, P680 shows rather weak excitonic coupling in the Qy excited state (*7*−*11*). The triplet state of P680 (^{3}P680) is localized on one Chl molecule at helium temperature, which is oriented almost parallel to the membrane plane (*12*) in contrast to the perpendicular orientation of bacterial P870 (*13*−*15*). Taking account of such information, various models of P680 have been proposed [reviewed in (*2, 16*)] including a monomer (*12*), a(n) (anti)parallel dimer (*17*−*19*), a T-shape dimer (*12, 20*), and a multimer (*21*). However, decisive conclusion on the P680 structure has not been obtained yet.

Light-induced FTIR difference spectroscopy is a powerful technique to investigate the structure and interaction of cofactors in photosynthetic proteins (*22, 23*). The FTIR difference spectra of P870 of purple bacteria (*24, 25*), P840 of green sulfur bacteria (*26, 27*), P798 of heliobacteria (*27, 28*), and P700 of photosystem I (*29*) upon their photooxidation have been detected, and their structures have been studied. In this study, we have measured a light-induced FTIR difference spectrum of P680 upon its photooxidation ($P680^+$/P680) in the frequency region of 1000−3000 cm^{-1}. To obtain the spectrum, we have used the RC complex (D1−D2−Cyt*b*559) of PS II in the presence of ferricyanide as an exogenous electron acceptor. The PS II RC complex typically includes six Chl, two Pheo, and two β-carotene molecules, while quinone acceptors of Q_A and Q_B are depleted in the preparation procedure (*16*). Since electron donation by Y_Z to $P680^+$ is also blocked in the RC complex, $P680^+$ can be easily photoaccumulated in the presence of artificial electron acceptors (*30*−*32*). In the obtained $P680^+$/P680 FTIR spectrum, we have found evidence that a positive charge on $P680^+$ is delocalized over (or hopping between) the Chl molecules. Also, from comparison with the ^{3}P680/P680 spectrum that we previously reported (*20*), it was suggested that the triplet state produced at low temperatures resides on a Chl molecule different from the Chls that possess a positive charge in $P680^+$. Based on these findings, we will discuss the structural model of Chl molecules coupled in the cation, triplet, and Qy singlet states.

MATERIALS AND METHODS

The RC complex of PS II (D1−D2−Cyt*b*559) was isolated from spinach as in ref (*33*) followed by replacement of the original detergent (Triton X-100) with 0.2% dodecyl maltoside. The RC sample was dissolved in 10 mM Hepes−NaOH buffer (pH 7.5) including 0.1% dodecyl maltoside and stored at −80 °C until use. For an H_2O/D_2O exchange experiment, the RC sample in the Hepes buffer (pH 7.5) was dried once under N_2 gas flow and dissolved in D_2O followed by incubation at 6 °C overnight. Further adjustment of pD was not performed. BBY-type PS II membranes (*34*) were prepared from spinach according to Ono and Inoue (*35*). The Mn-cluster was depleted by NH_2OH treatment as in ref (*36*).

Light-induced FTIR difference spectra were measured on a JEOL JIR 6500 spectrophotometer equipped with an MCT detector (EG&G JUDSON IR-DET101) with 4 cm^{-1} resolution as described previously (*37*). For $P680^+$/P680 measurement, 12 μL of RC sample (1.4 mg of chlorophyll/mL) was cast on a BaF_2 plate (13 mm ϕ) and lightly dried under N_2 gas flow. The obtained film was then wetted with 1 μL of 100 mM sodium ferricyanide solution and briefly dried. The sample was then covered with another BaF_2 plate. The sample temperature was adjusted to 150 K in a cryostat (Oxford DN1704) with a controller (Oxford ITC-4). Difference spectra were obtained by subtraction between the two single-beam spectra (200 scans: 100 s accumulation for each spectrum) recorded before and under continuous-light illumination. The light source was a halogen lamp equipped with heat-cut and red (>600 nm) filters (~20 mW/cm^2 at the sample). Light illumination at 250 K to bleach β-carotene was performed in the cryostat using the same light source. Each final spectrum was an average of two spectra, which were measured with the same sample. Between the two measurements, the sample was incubated at 278 K to relax the charged species. Before taking an average, it was ascertained that the first and the second spectra were identical. For examining the thermal effect of light illumination on the difference spectra, the RC sample without any artificial electron acceptor was used. All the other measuring conditions were the same as those for the measurements in the presence of ferricyanide.

The Chl_Z^+/Chl_Z FTIR difference spectrum was obtained at 210 K using Mn-depleted PS II membranes in the presence of a mixture of ferricyanide and silicomolybdate as exogenous electron acceptors as described in ref (*36*). For detecting the spectrum in the frequency region higher than 1700 cm^{-1}, the sample was loaded with an about 3 times larger amount than for the lower frequency region, to diminish the influence of background fluctuation.

Electronic absorption spectra at 300−1200 nm were measured on a Shimadzu UV-3100PC spectrophotometer with 1 nm resolution. Sample preparation for measurements, the cryostat system, and the light source for illumination were the same as those used for the FTIR measurements except that a half amount of sample was loaded to avoid band saturation. For obtaining a difference spectrum of after-minus-before illumination, the spectrum measured before illumination was subtracted from that after 40 s illumination. For spectra under illumination and the time course at 682 and 1004 nm, the incident light was passed through a combination of a blue band-pass filter (Toshiba B-57) and a cold filter (Nihon Shinku Kogaku type-B), and the detector was protected by a red filter (Toshiba R-60).

Resonance Raman (RR) spectra were measured with a JASCO TRS-600/S monochromator equipped with an 1800 groove/mm grating. Laser lines at 406.7 nm from a Kr ion laser (Coherent, Innova 90-K) and at 441.6 nm from a He−Cd laser (Kimmon IK5651R-G) were used for excitation, and Raman scattering was collected perpendicular to the laser beam. The dispersed Raman scattering was detected with a

CCD detector (Princeton Instruments, Inc., LN/CCD-1100PBUVAR). Rayleigh scattering was removed with a holographic Notch filter (Kaiser Optical Systems, Inc.). The RC complex (0.2 mg of chlorophyll/mL) in 50 mM Hepes−NaOH buffer (pH 7.5) including 0.1% dodecyl maltoside was placed in a glass cell, and the temperature was kept at 85 K in a cryostat (Oxford DN1704). The laser power was about 15 mW at the sample point for both laser lines, and the laser beam was defocused to prevent sample degradation. One spectrum was accumulated for 1 h, and then the beam spot on the sample was shifted for another measurement. Three and four spectra were averaged for obtaining the final spectra of 406.7 and 441.6 nm excitation, respectively. Spectral resolution was about 4 cm^{-1}.

RESULTS

Electronic Absorption Spectra in the 300−1200 nm Region. Figure 1 shows an electronic absorption spectrum (300−1200 nm) of the PS II RC complex (a) and its light-induced difference spectra (b−d). The sample was the same as that used for FTIR measurements (see below), i.e., a lightly dried RC film that includes ferricyanide as an exogenous electron acceptor. The absorption spectrum measured at 150 K before light illumination (Figure 1a) was basically identical to the spectrum in the literature (*16*). In particular, the split peaks of the Qy band at 673 and 678 nm are typical of the PS II RC complex at low temperatures (*38*−*40*).

Light illumination of the RC sample at 150 K provided the difference spectra shown in Figure 1b and Figure 1b′. The spectrum of after-minus-before illumination was obtained in the whole region (Figure 1b), while only the Qy region was shown for the difference spectrum measured under illumination (Figure 1b′). In both cases, a prominent negative peak at 682 nm with a shoulder at 673 nm was observed in the Qy region. Previously, Telfer and Barber (*31*) reported an almost identical light-induced difference spectrum in the Qy region, which showed a main peak at 680 nm with a 672 nm shoulder, using silicomolybdate as an electron acceptor, and attributed the main peak to the bleach of P680 due to photoaccumulation of its cation and the shoulder to additional oxidation of monomeric Chl. Also, by illumination of the RC complex with silicomolybdate or ferricyanide at cryogenic temperatures, a narrow EPR signal (0.8 mT) from $P680^+$ as well as another signal (1 mT) from an oxidized monomeric Chl was observed (*30*, *32*). Therefore, bleaching of the Qy bands in Figure 1b,b′ can be interpreted as formation of $P680^+$ (682 nm) concomitant with minor oxidation of an accessory Chl (673 nm).

The presence of negative peaks at 508, 476, and 440 nm and a large positive peak at 1004 nm (Figure 2b) indicates that β-carotene in the RC complex was also oxidized by illumination and its radical cation was accumulated (*37*, *41*). It has been reported that two distinct β-carotene molecules are attached to the RC complex: one with peaks at 489, 458, and 429 nm and the other at 507, 473, and 443 nm (*42*, *43*). From the wavelength positions of bleached bands in Figure 1b, the latter β-carotene molecule seems to be specifically oxidized by $P680^+$. The spectrum in Figure 1b could be repeatedly obtained with the same intensity by incubating the sample at 278 K between the measurements, indicating

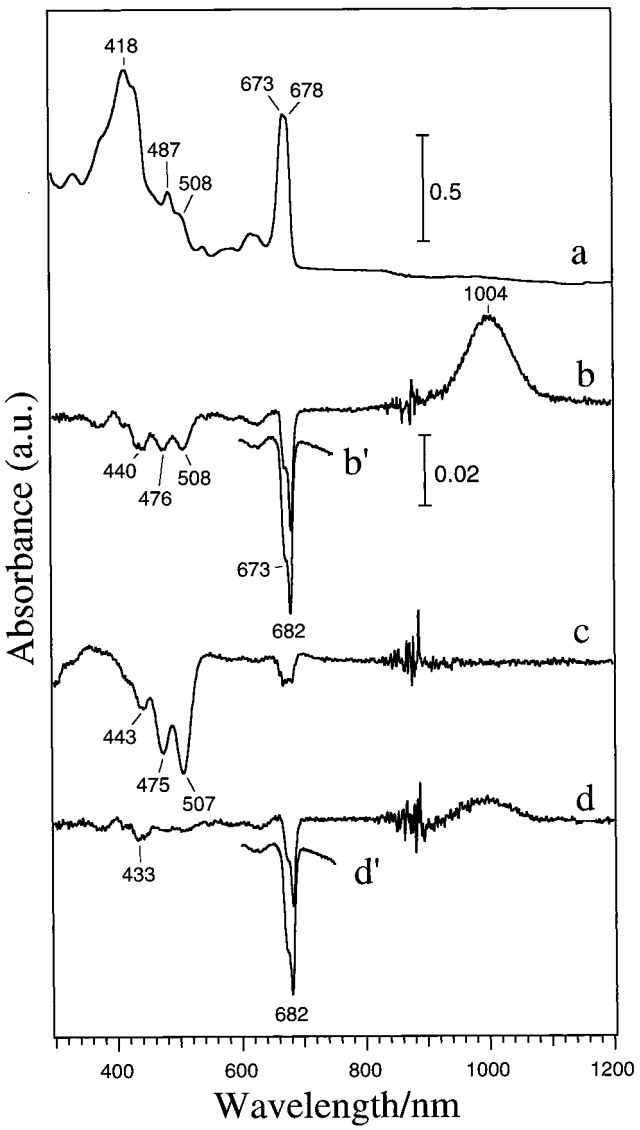

FIGURE 1: Electronic absorption spectrum (300−1200 nm) of the PS II RC complex in the presence ferricyanide (a) and its light-induced difference spectra (b−d). (a) Absorption spectrum measured at 150 K before illumination. (b) Difference spectrum between before and after illumination (40 s) measured at 150 K and that between before and under illumination (b′). (c) Difference spectrum between before and after illumination (30 min) measured at 250 K. The RC sample after the measurement of spectrum b was once incubated at 278 K to relax the charged species and then cooled to 250 K. (d) Difference spectrum between before and after illumination (40 s) measured at 150 K using the 250 K-preilluminated sample (sample after the measurement of spectrum c), and that between before and under illumination (d′). Spectral resolution was 1 nm. The detector was changed at 890 nm from PbS (for longer wavelengths) to a photomultiplier (for shorter wavelengths).

that no irreversible change occurred on the RC sample by illumination at 150 K and the produced radical species were fully relaxed at 278 K.

The time course of the bleached band of P680 at 682 nm and the positive band of the carotenoid cation at 1004 nm was measured at 150 K (Figure 2). Upon illumination, the bleach of P680 and the appearance of the carotenoid cation occurred almost with the same rate. When the light was turned off, the carotenoid cation at 1004 nm showed only slow relaxation, whereas the 682 nm band showed double phase relaxation with a relatively fast rate ($t_{1/2} = \sim 1$ min) and a very slow rate. Since the band shape of the Qy bleach

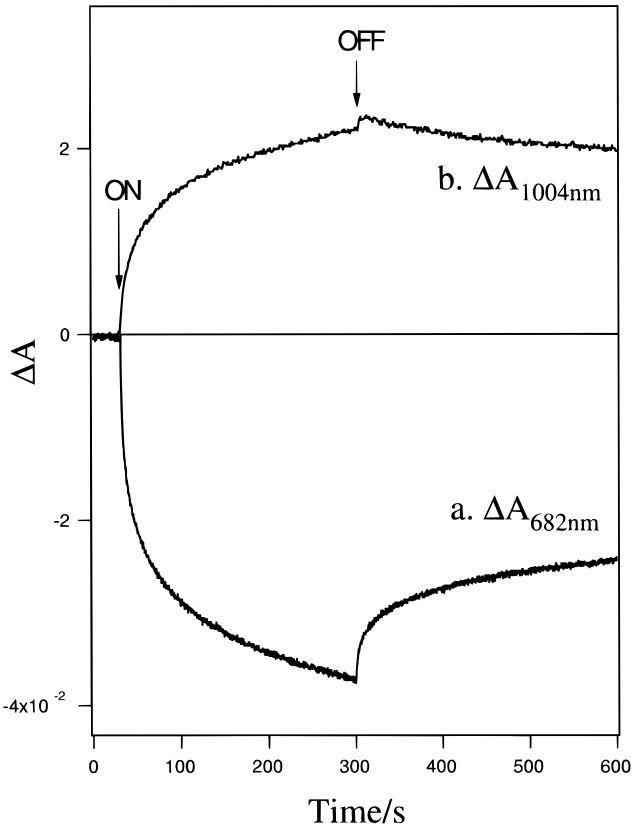

FIGURE 2: Time course of the light-induced absorption changes at 682 nm (a) and 1004 nm (b). Timing of starting and stopping the illumination is indicated by 'ON' and 'OFF', respectively.

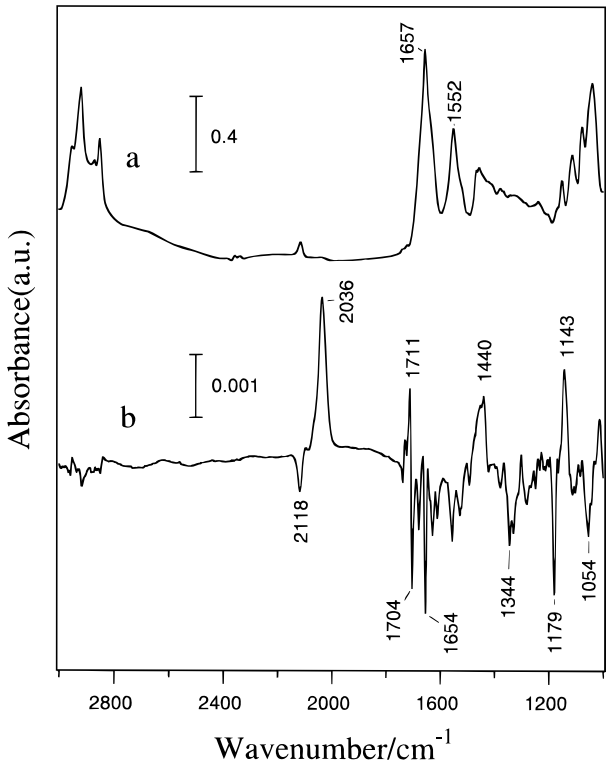

FIGURE 3: FTIR spectrum (1000−3000 cm^{-1}) of the PS II RC complex in the presence of ferricyanide before illumination (a) and its light-induced difference spectrum (under-minus-before illumination) (b). The sample temperature was 150 K. Spectral resolution was 4 cm^{-1}.

was basically the same between under and after illumination except a slightly higher shoulder at 673 nm under illumination (Figure 1b), this double phase relaxation may be brought about by heterogeneity of the state of the RC complex regarding the electron donor, e.g., the distance between P680 and ferrocyanide in the RC complex.

After the experiment at 150 K for Figure 1b, the sample was incubated at 278 K to relax the photoproduced charged species, and then the temperature was adjusted to 250 K. At this temperature, the RC sample was illuminated for 30 min, and a difference spectrum of after-minus-before illumination was obtained (Figure 1c). The spectral feature was significantly different from that observed at 150 K (Figure 1b). Negative peaks at 507, 475, and 443 nm due to β-carotene were prominent, but the corresponding positive peak of the carotenoid cation at 1004 nm was not observed. In the Qy region, only minor bleach of Chl molecules was seen at 670−680 nm. From the positions of the three negative peaks of the carotenoid (Figure 1c), it is considered that the β-carotene molecule, which was photooxidized and stably stayed in the cation form at 150 K (Figure 1b), was specifically bleached at 250 K. The band shape of the bleached carotenoid was rather unusual; i.e., the 0−0 peak at 507 nm was larger than the 0−1 peak at 475 nm (Figure 1c), indicating that some absorption bands appeared overlapping the bleached bands. However, no carotenoid species other than β-carotene was found, when the pigment extract from this 250 K illuminated RC sample was subjected to thin-layer chromatography. Probably, in part of the RC complexes, the β-carotene molecule that escaped from degradation was released from its binding pocket to cause a blue shift. It is noted that the above reaction is not specific to the film sample used in this experiment, but the same difference spectrum was observed by using a solution sample in the presence of ferricyanide.

Following the illumination at 250 K, the sample was cooled to 150 K, and light-induced difference spectra were measured under the same conditions as for Figure 1b,b′. The obtained spectra are shown in Figures 1d (after-minus-before illumination) and 1d′ (under-minus-before illumination). The prominent difference of Figure 1d from Figure 1b is that the negative bands due to carotenoid at 508, 476, and 440 nm and the positive band of its cation at 1004 nm dramatically diminished. In contrast, in the Qy region, the band shape of a negative peak at 682 nm with a shoulder at 673 nm did not change although a little decrease in intensity was observed. The identical spectrum was obtained even when the 250 K-illuminated sample was incubated at 278 K before cooling down to 150 K, indicating that specific bleaching and release of β-carotene at 250 K are irreversible reactions. Thus, this 250 K-preilluminated RC sample is useful to measure an FTIR difference spectrum of P680 with little interference of carotenoid signals.

FTIR Spectra. Figure 3 shows an FTIR spectrum (1000−3000 cm^{-1}) of the untreated PS II RC complex in the presence of ferricyanide in the dark (a) and its light-induced difference (under-minus-before illumination) spectrum (b) measured at 150 K. Similar difference spectra were obtained in the temperature range of 77−210 K (data not shown). A change from ferricyanide to ferrocyanide was shown in the bands at 2118/2036 cm^{-1}, indicating that an electron was abstracted by ferricyanide through Pheo and hence a positive charge was accumulated on the electron donor side. Ac-

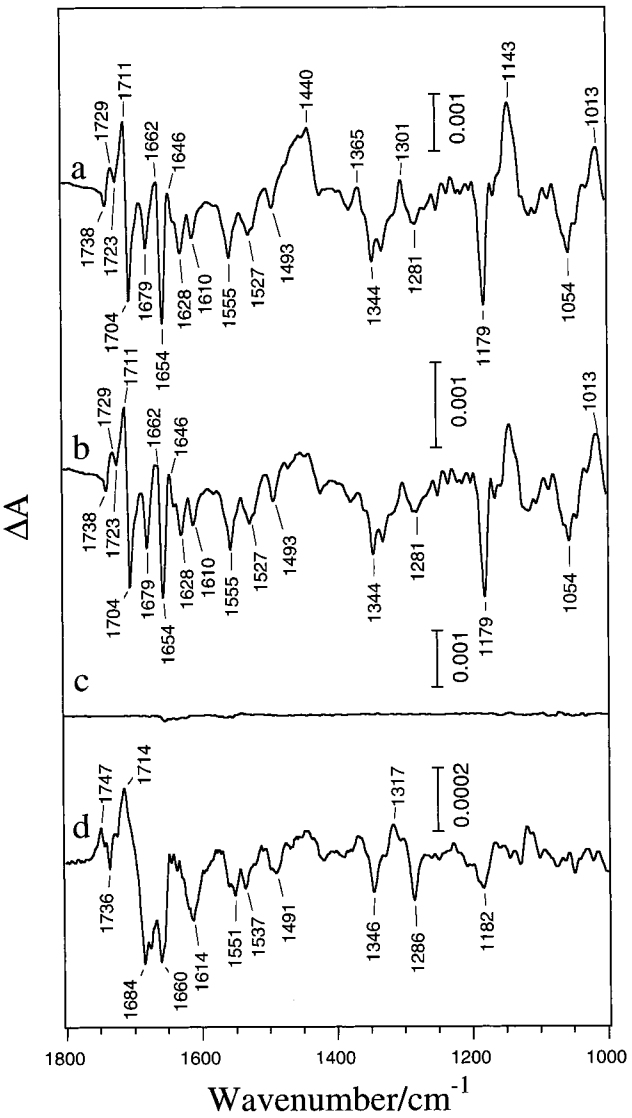

FIGURE 4: Light-induced FTIR difference spectra in the lower frequency region (1000−1800 cm^{-1}) of the PS II RC complex (a−c) and the Mn-depleted PS II membranes (d). (a) Difference spectrum (under-minus-before illumination) of the RC complex in the presence of ferricyanide, representing $P680^+$carotenoid$^+$/P680carotenoid. The spectrum was measured at 150 K. (b) Difference spectrum (under-minus-before illumination) of the RC complex after specific bleach of β-carotene, representing $P680^+$/P680. The sample was preilluminated for 30 min at 250 K to bleach β-carotene. The spectrum was measured at 150 K. (c) Light-induced difference spectrum (under-minus-before illumination) of the RC complex without exogenous electron acceptors. Measuring condition was the same as for spectrum a. (d) Difference spectrum (after-minus-before illumination) of the Mn-depleted PS II membranes in the presence of ferricyanide and silicomolybdate, representing Chl_Z^+/Chl_Z (*36*). The spectrum was measured at 210 K.

cording to the above result of electronic absorption spectra (Figure 1b), $P680^+$ and a radical cation of β-carotene should be mainly produced with minor contribution of the cation of an accessory Chl. It is notable that in addition to a number of bands present in the 1000−1750 cm^{-1} region, a broad, weak feature is observed at 1700−2800 cm^{-1} (Figure 3b).

The lower frequency region (1000−1800 cm^{-1}) of the difference spectrum (Figure 3b) is expanded in Figure 4a, and an analogous light-induced difference spectrum measured using a 250 K-preilluminated RC sample is shown in Figure 4b. In the latter spectrum, the bands at 1440, 1365, and 1143 cm^{-1} significantly decreased their intensities compared with those in the spectrum of the untreated RC sample (Figure 4a). Because β-carotene is specifically bleached by pre-illumination at 250 K (Figure 1c), this observation indicates that the bands at 1440, 1365, and 1143 cm^{-1} arise from a radical cation of β-carotene. The bands at 1440 and 1143 cm^{-1} may correspond to the doublet signal at 1465 and 1441 cm^{-1} and the 1148 cm^{-1} band, respectively, which were previously reported for a β-carotene cation photoproduced in the PS II membranes at 80 K (*37*). The difference in the band shape and positions may reflect some perturbation of carotenoid configuration and/or interaction with surrounding proteins in the RC complex from an intact state. Note that the reason no corresponding negative bands of a neutral carotenoid were observed in the spectrum, is that a neutral carotenoid has much weaker IR bands than its cation state (*37*). With minimum contribution of carotenoid signals, we can regard the spectrum in Figure 4b as the $P680^+$/P680 difference probably with some contamination of the signals from an accessory Chl.

Because in the measurements of the above FTIR difference spectra relatively long light illumination (100 s) was subjected to the sample, there could be a risk of contamination of thermal bands, which come from subtle frequency shifts of various vibrational modes in the whole system due to the temperature increase through light absorption of the pigments and subsequent thermal relaxation. To check the thermal effect on the spectra, we measured a light-induced spectrum of the PS II RC complex in the absence of exogenous electron acceptors under the same conditions as used for Figure 4a,b. In such a sample, the triplet formation and subsequent relaxation (∼1 ms) occur (*44*), and thus the temperature increase by illumination should be even larger than the case of the presence of an electron acceptor. As seen in Figure 4c, thermal bands showed almost no intensities in the scale of the $P680^+$/P680 spectrum (Figure 4a,b). It should be noted that although we previously detected a triplet signal with relatively large contamination of thermal bands under similar conditions (a RC sample without acceptors) (*20*), the intensity of the incident light was 25 times higher (to accumulate a short-lived triplet) in that experiment than that used in the present study.

In PS II there is a Chl molecule, so-called Chl_Z, which works as a peripheral electron donor to $P680^+$ at cryogenic temperatures when the Mn-cluster is depleted. We previously measured a light-induced FTIR difference spectrum of Chl_Z upon its photooxidation at 210 K using Mn-depleted PS II membranes (*36*). This Chl_Z^+/Chl_Z spectrum is presented in Figure 4d compared with the $P680^+$/P680 spectrum (Figure 4b). The overall spectral feature is similar between the two spectra, and most of the bands correspond well with each other. In the C═O stretching region (1600−1750 cm^{-1}), where C═O groups of Chl, amide I modes of polypeptides, and COOH groups of side chains mainly contribute, relatively large negative bands are observed at 1704, 1679, and 1654 cm^{-1} in the $P680^+$/P680 spectrum (Figure 4b), while similar bands are observed at 1684 and 1660 cm^{-1} in the Chl_Z^+/Chl_Z spectrum (Figure 4d). Positive bands appear at 1711 and 1729 cm^{-1} in $P680^+$/P680 corresponding to the bands at 1714 and 1747 cm^{-1} in Chl_Z^+/Chl_Z. The tendency of the presence of the positive bands at higher frequencies than the negative bands follows the fact

that both the keto C_9═O and carbomethoxy C_{10}═O bands of Chl upshift upon its cation formation (*29*). It should be noted that despite the overall similarities, the C═O frequencies of the Chl_Z^+/Chl_Z spectrum agree with none of the bands in the $P680^+/P680$ spectrum. This means that the accessory Chl included in the $P680^+/P680$ spectrum as contamination is not Chl_Z. Oxidation of Chl_Z by $P680^+$ may be blocked in the RC preparation. This blockage of Chl_Z oxidation as well as the blockage of Y_Z oxidation may be the reason in the RC protein $P680^+$ is mainly photoaccumulated in contrast to the formation of Chl_Z^+ in the membrane preparation under similar illumination conditions.

The bands assignable to the macrocycle C═C stretching modes of neutral Chl (*45*−*47*) are observed at 1610, 1555, 1527, and 1493 cm^{-1} in $P680^+/P680$ (Figure 4b), corresponding to 1614, 1551, 1537, and 1491 cm^{-1} in Chl_Z^+/Chl_Z (Figure 4d). Some of these modes can be used as marker bands to identify the coordination number of the central Mg ion of Chl (*45, 48*); IR bands at ∼1610 and ∼1535 cm^{-1} in 5-coordinated Chl downshift to ∼1600 and ∼1515 cm^{-1}, respectively, in 6-coordinated Chl. The presence of bands at 1610 and 1527 cm^{-1} in $P680^+/P680$ (Figure 4b) indicates that the Chl molecules in P680 have a 5-coordinated structure.

Other prominent ring modes of neutral Chl, that consist of CC and CN stretching and CH bending vibrations (*47*), are observed at 1344, 1281, and 1179 cm^{-1} in $P680^+/P680$ (Figure 4b), corresponding to the bands at 1346, 1286, and 1182 cm^{-1} in Chl_Z^+/Chl_Z (Figure 4d). The notable difference between the two spectra in this region is observed in the band intensities; in P680, the 1179 cm^{-1} band shows a significantly strong intensity, while in Chl_Z all three bands have about the same minor intensities. An FTIR difference spectrum of a monomeric Chl in vitro upon cation formation (*29, 49*) also showed the corresponding three bands at 1346, 1289, and 1179 cm^{-1} with minor intensities.

The higher frequency region (1700−2800 cm^{-1}) of the light-induced difference spectra (under-minus-before illumination) of the untreated and 250 K-preilluminated RC samples is presented in Figure 5a,b, respectively (different spectral region of Figure 4a,b). A light-induced spectrum of the RC sample without ferricyanide is also shown in Figure 5c, demonstrating that the thermal effect by illumination does not contribute to the spectra in this region either. In both the spectra of Figure 5a and Figure 5b, a broad band centered at ∼1940 cm^{-1} with a width (fwhm) of 430 ± 30 cm^{-1} was observed. Peaks at 2623, 2440, and 2290 cm^{-1} were also seen on the broad band, but these peaks decreased their intensities in the 250 K-preilluminated RC (Figure 5b). In a difference spectrum of the untreated RC taken *after* illumination (not shown), the broad band as well as the bands at 1000−1750 cm^{-1} (except for the bands at 1440, 1365, and 1143 cm^{-1}) became smaller without changing the intensities of the peaks at 2623, 2440, and 2290 cm^{-1}. This observation corresponds to the partial fast relaxation of $P680^+$ and the very slow relaxation of the β-carotene cation (Figure 2). Therefore, the peaks at 2623, 2440, and 2290 cm^{-1} are assigned to the β-carotene cation, and the broad band can be ascribed to $P680^+$. These carotenoid bands probably arise from overtones and/or combination modes. The broad band centered at 1940 cm^{-1} resembles the mid-IR electronic band of bacterial P^+, which has been reported at ∼2600 cm^{-1} (fwhm: 730 ± 50 cm^{-1} at 100 K) in purple bacteria (*25*), at ∼2500 cm^{-1} (fwhm: 570 ± 30 cm^{-1} at 150 K) in green sulfur bacteria (*26, 27*), and at ∼2100 cm^{-1} [fwhm: ∼800 cm^{-1} taken from Figure 2 in ref (*28*) (220 K)] in heliobacteria. This electronic band of bacterial P^+ has been considered to arise from charge delocalization (or hopping of a hole) on the BChl dimer (*25, 50*−*52*). The broad band of $P680^+$ shows a weaker intensity compared with the mid-IR electronic band of bacterial P^+: about 10 times weaker

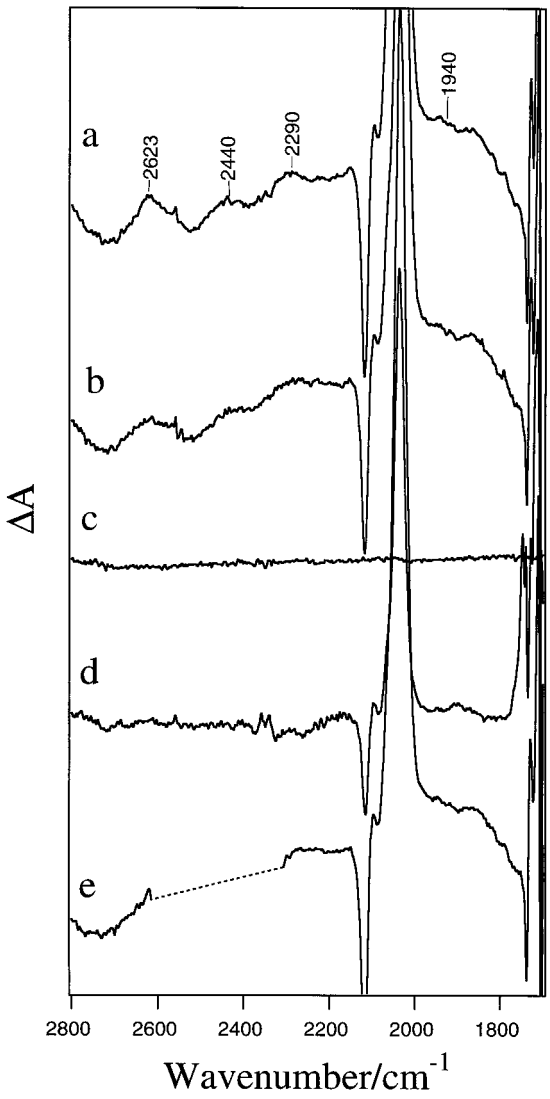

FIGURE 5: Light-induced FTIR difference spectra in the higher frequency region (1700−2800 cm^{-1}) of the PS II RC complex (a−c, e) and the Mn-depleted PS II membranes (d). Spectra a−c are the different frequency region of the spectra in Figure 4a−c. (a) Difference spectrum of the RC complex in the presence of ferricyanide, representing $P680^+$carotenoid$^+$/P680carotenoid. The spectrum was measured at 150 K. (b) Difference spectrum of the RC complex after specific bleach of β-carotene (preilluminated at 250 K), representing $P680^+/P680$. The spectrum was measured at 150 K. (c) Difference spectrum of the RC complex without exogenous electron acceptors. The spectrum was measured at 150 K. (d) Difference spectrum of the Mn-depleted PS II membranes in the presence of ferricyanide and silicomolybdate, representing Chl_Z^+/Chl_Z. Measuring condition was the same as for Figure 4d, except that an about 3 times larger amount of sample was loaded. (e) Difference spectrum of the RC complex in D_2O buffer in the presence of ferricyanide. Measuring condition was the same as for spectrum a. The spectral region connected by a dotted line is saturated by a D_2O band.

than that of P^+ of purple and green bacteria (*25*−*27*) and about 3 times weaker than that of heliobacteria (*27*, *28*) on the basis of the spectral intensity in the C═O region.

The same spectral region of the Chl_Z^+/Chl_Z difference spectrum is shown in Figure 5d. This spectrum was normalized so as to adjust the intensity of the C═O band at 1747 cm^{-1} to that of the 1729 cm^{-1} band of Figure 5a,b. Note that the relative intensity of the 1747 cm^{-1} band in the whole C═O region (Figure 4d) is about the same as that of the 1729 cm^{-1} band of $P680^+/P680$ (Figure 4a,b). The broad band was not observed in this Chl_Z^+/Chl_Z spectrum, being consistent with the idea that Chl_Z is one of the monomeric accessory Chl molecules in the RC complex (*53*).

A broad continuum in a higher frequency region can arise from strong hydrogen bond interactions with large proton polarizability (*54*, *55*). Hence, there is a possibility that the broad feature in $P680^+/P680$ comes from an effect of the electric field change or some structural perturbation on the hydrogen bond interactions around P680. To check this possibility, a $P680^+/P680$ difference spectrum was measured using the RC sample incubated in D_2O buffer (Figure 5e). The broad band centered at 1940 cm^{-1} was still observed with basically the same shape, supporting the idea that this band is an electronic band of $P680^+$. Since P680 is thought to be present in a hydrophobic environment, hydrogen-bonding protons may not be exchanged by simple incubation in D_2O buffer. Hence, the possibility that the broad band comes from hydrogen-bonding interactions cannot be fully excluded. However, from the resemblance to the bacterial mid-IR electronic band and the result that Chl_Z did not show this feature upon its cation formation (Figure 5d), which should similarly perturb hydrogen-bonding interactions around Chl_Z, it can be concluded that the broad band centered at ∼1940 cm^{-1} of $P680^+$ arises from an electronic transition of dimeric Chl molecules.

Comparison with RR Spectra and a Triplet/Singlet FTIR Spectrum. To understand the origin of the C═O bands in more detail, RR spectra of the RC complex were measured and compared with the FTIR spectrum. In Figure 6, RR spectra measured with excitation at 406.7 (a) and 441.6 nm (b) were presented together with the $P680^+/P680$ FTIR spectrum (c) (expansion of Figure 4b). These RR spectra were basically identical to the spectra previously reported by Moënne-Loccoz et al. (*56*) except that the spectral resolution seems a little higher in the present study and thus the bands at 1722−1725 cm^{-1} are resolved in Figure 6a,b. While the $P680^+/P680$ FTIR spectrum includes the bands of not only P680 itself but also the surrounding molecules such as proteins and other pigments that are perturbed by $P680^+$ formation, the RR spectra provide only the vibrational modes of pigments that are resonant to the excitation wavelength. In the case of PS II RC, the six Chl and two Pheo molecules have almost degenerate Soret absorption bands at 400−450 nm (Figure 1a), and hence RR spectra measured with excitation in the Soret region will include basically all the contribution of these chlorin molecules in the RC complex. Since the 418 nm peak (Figure 1a) is due to Pheo, the spectrum with 406.7 nm excitation might include more Pheo contribution. However, since we do not know the exact position of the Soret band of P680 and in addition P680 might show a specific resonance effect, it is also possible that the difference between the RR spectra with

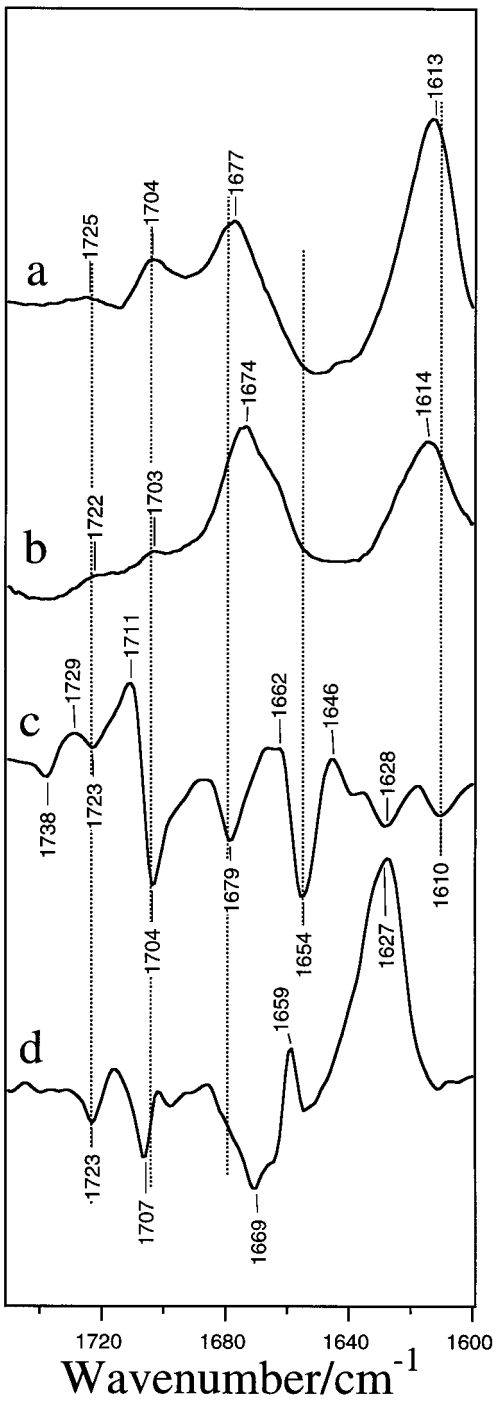

FIGURE 6: Resonance Raman spectra of the PS II RC complex in the C═O and C═C regions measured with excitation at 406.7 (a) and 441.6 nm (b), in comparison with FTIR difference spectra of $P680^+/P680$ (expanded spectrum of Figure 4b) (c) and of triplet/singlet [taken from ref (20), in which the spectrum was reported as $^3P680/P680$] (d). For resonance Raman measurements, the RC complex was dissolved in 50 mM Hepes−NaOH buffer (pH 7.5) (0.2 mg of chlorophyll/mL) without exogenous electron acceptors and kept at 85 K in a cryostat. Spectral resolution was about 4 cm^{-1}.

406.7 and 441.6 nm excitation (Figure 6a,b, respectively) reflects the P680 contribution.

The C═C stretching mode of the Chl macrocycle was observed at 1613−1614 cm^{-1} in both the RR spectra (Figure 6a,b), confirming the assignment of the FTIR band at 1610 cm^{-1} (Figure 6c) to the C═C mode. Because the negative peak at 1628 cm^{-1} in the $P680^+/P680$ FTIR spectrum (Figure

6c) does not have a counterpart in the RR spectra (Figure 6a,b), this band is probably ascribed to a protein mode, either an amide I or a side chain mode.

RR bands at 1660−1710 cm^{-1} (Figure 6a,b) can be assigned to the keto C_9═O stretching modes of Chl and Pheo (*45*, *46*). These bands are classified into two groups, i.e., the higher frequency bands with a peak at 1703−1704 cm^{-1} and the lower frequency bands with a peak at 1674−1677 cm^{-1} and a shoulder at ∼1665 cm^{-1}. The former group is attributed to the C_9═O free from hydrogen bonding, and the latter group is to the hydrogen-bonded C_9═O (*57*−*59*). The large negative band at 1654 cm^{-1} in the $P680^+$/P680 FTIR spectrum (Figure 6c) definitely originates from neither Chl nor Pheo, because no C═O band exists at this position in the RR spectra (Figure 6a,b). Hence, this 1654 cm^{-1} band is assigned to the protein mode. The most plausible assignment is the amide I mode of an α-helical polypeptide, which generally shows a band at 1650−1658 cm^{-1} (*60*). This assignment is reasonable because P680 is thought to be attached to the transmembrane α-helices (*1*, *19*). The positive peaks at 1662 and 1646 cm^{-1} might be counterparts of the 1654 cm^{-1} negative band. The negative bands at 1679 and 1704 cm^{-1} of the $P680^+$/P680 FTIR spectrum (Figure 6c) are most likely due to the keto C_9═O modes of Chl or Pheo, because these positions are in good agreement with the keto C_9═O bands in the RR spectra (Figure 6a,b). At least one of them must be attributed to the keto C_9═O of P680. However, definite assignment is difficult at present, because of (1) contamination of the signals of an accessory Chl represented by a shoulder at 673 nm in the Qy region (Figure 1b,d), (2) possible electrochromic effect on the C═O bands of other Chl or Pheo molecules near P680, and (3) possible contribution of protein bands (amide I or side chains).

It is known that the keto C_9═O frequency upshifts by about 25 cm^{-1} when Chl in THF is oxidized (*29*). If the positive charge is delocalized on dimeric Chl molecules, the shift is expected to be smaller. Thus, the positive bands at 1711 and 1729 cm^{-1} (Figure 6c) can be the candidates for the keto C_9═O bands of $P680^+$. The carbomethoxy C_{10}═O of Chl and Pheo, which generally shows a stretching frequency at 1720−1750 cm^{-1} (*59*), is only weakly conjugated to the chlorin ring, and hence significantly low RR intensity is expected. In fact, only one weak band was observed at 1722−1725 cm^{-1} in the RR spectra (Figure 6a,b). This band position indicates that the carbomethoxy C_{10}═O group is hydrogen-bonded (*59*). Since it is unlikely that all the carbomethoxy C_{10}═O groups of eight chlorin molecules in the RC complex are engaged in hydrogen bonds, only some of them must have gained RR intensities with unknown reason. A dip at 1723 cm^{-1} in the $P680^+$/P680 FTIR spectrum (Figure 6c) might correspond to this RR band. If this is the case, the counterpart of this dip in the $P680^+$ spectrum could be the 1729 cm^{-1} band, because oxidation of Chl slightly upshifts the carbomethoxy C_{10}═O frequency (*29*). Another negative peak was found at 1738 cm^{-1} in $P680^+$/P680 (Figure 6c), but the counterpart of this peak was not clear in the spectrum. The C═O stretching mode of a COOH group of Asp or Glu also shows a band in this region (1700−1750 cm^{-1}), and thus this side-chain mode might also contribute to the above peaks.

The $P680^+$/P680 difference spectrum (Figure 6c) was also compared with the triplet/singlet spectrum (Figure 6d) measured at 80 K, which we previously reported as ^{3}P680/P680 (*20*). In this triplet/singlet spectrum, the main bleach of the keto C_9═O band of the Chl in the ground singlet state is observed at 1669 cm^{-1} with a minor bleach at 1707 cm^{-1}. The positive bands at 1627 and 1659 cm^{-1} were ascribed to the C_9═O bands of the triplet Chl as counterparts of the 1669 and 1707 cm^{-1} bands, respectively. It is clearly seen that the main C_9═O band at 1669 cm^{-1} agrees with neither the 1704 cm^{-1} nor the 1679 cm^{-1} band in the $P680^+$/P680 spectrum. This observation automatically leads to the conclusion that the Chl molecule on which the triplet state is mainly located at low temperatures is different from the Chl molecules that possess a hole in $P680^+$. By contrast, the minor band at 1707 cm^{-1} in the triplet/singlet spectrum (Figure 6d) could correspond to the 1704 cm^{-1} band in the $P680^+$/P680 spectrum (Figure 6c). In this case, the slight frequency difference by 3 cm^{-1} is possibly brought about by the overlap of other bands (especially a positive band at 1711 cm^{-1} in Figure 6c) or the difference in the measuring condition (e.g., temperature and presence of an electron acceptor).

DISCUSSION

Identification of a $P680^+$/P680 FTIR Spectrum. Previously, Allakhverdiev et al. (*61*) claimed that they obtained a $P680^+$/P680 FTIR spectrum at 20 °C using Mn-depleted PS II membranes in the presence of ferricyanide and silicomolybdate as electron acceptors. However, their spectrum is at odds with our $P680^+$/P680 spectrum (Figure 4b) in the present study. The band pattern of their spectrum is quite different from that of a typical Chl spectrum, which has been seen in Chl^+/Chl in vitro (*29*), Chl_Z^+/Chl_Z in PS II (Figure 4d) (*36*), and $P700^+$/P700 in PS I (*29*), whereas overall features and band positions of our $P680^+$/P680 spectrum (Figure 4b) correspond well to those of Chl_Z^+/Chl_Z (Figure 4d) (*36*) as well as other published Chl spectra (*29*). The intensity of their difference spectrum (ΔA) was about 0.05 [which was estimated from Figure 3 in ref (*61*) by assuming the absorbance of the amide I band as 1]. However, using PS II membranes, the predicted spectral change is on the order of 10^{-4}, which is the spectral scale of light-induced difference spectra of various species so far obtained using PS II membranes (*36*, *37*, *62*−*69*). By contrast, the scale of our spectrum is quite reasonable. Taking into consideration the number of backbone C═O groups in the RC protein (∼850) as well as some contribution of side chains and chlorin pigments, the intensity ratio of the C═O bands of P680 to the total bands in the amide I region (1600−1700 cm^{-1}) can be expected to be about 1×10^{-3}. In fact, this is the spectral scale of our difference spectrum (Figure 3). Even when we calculate a ratio with area intensity, the sum of the negative bands at 1704 and 1679 cm^{-1}, candidates for the keto C_9═O of P680, in the difference spectrum (Figure 3b), was estimated to be about 4×10^{-4} of the amide I band at 1657 cm^{-1} of the original spectrum (Figure 3a). This value is reasonably explained, if $P680^+$ is photoaccumulated in about half the RC proteins during the FTIR measurement. Furthermore, we repeated the experiment by Allakhverdiev et al. (*61*) under basically identical conditions, but actually we obtained a spectrum

consisting of a mixture of the known signals of Chl_Z^+/Chl_Z (*36*) and Q_A^-/Q_A (*62*) (data not shown). Although we do not know the origin of their signals, it might be possible that they observed an artifact such as protein degradation.

Very recently, Breton et al. (*49*) reported their preliminary FTIR spectrum of $P680^+/P680$ in the 1150−1800 cm^{-1} region measured at 230 K using the PS II RC complex in the presence of silicomolybdate as an electron acceptor. Our spectrum in this lower frequency region (Figure 4b) was basically identical to their spectrum. The slight frequency differences (<5 cm^{-1}) observed in some of the bands might be due to the difference in temperature (150 K vs 230 K) and an electron acceptor. Observation of the basically identical spectra in independent laboratories using different RC preparations as well as some different measuring conditions (e.g., temperature and an electron acceptor) corroborates the correctness of the $P680^+/P680$ FTIR spectrum presented in this study.

Electronic Coupling and Structure of P680$^+$. In the $P680^+/P680$ FTIR spectrum, a relatively weak, broad band centered at 1940 cm^{-1} was observed (Figure 5a,b,e). Similar bands have been reported in various bacterial P^+ (*25*−*28*), and ascribed to an electronic transition originating from charge delocalization or hopping between the two BChl molecules (*25, 50*−*52*). In fact, this band was not observed in the cation state of a monomeric BChl in organic solution, an asymmetric dimer in bacterial mutants that has a BPheo in place of either of the BChl molecules (*25*), and Chl_Z in PS II (Figure 5d) that is thought to be a monomeric accessory Chl (*53*). Therefore, the presence of a mid-IR electronic band in $P680^+$ provides evidence that $P680^+$ has a dimeric structure consisting of electronically coupled Chl molecules and the positive charge is delocalized over (or hopping between) the two Chls. This conclusion is consistent with the ENDOR results by Rigby et al. (*32*), which indicated that an unpaired electron spin is delocalized over two Chl molecules with a ratio of 82:18, although they could not rule out the possibility of a monomeric structure in which environmental and geometrical changes affected the hyperfine coupling constants.

The intensity of the mid-IR electronic band observed in $P680^+$ (Figure 5a,b) was much lower than the corresponding band of bacterial P^+ (*25*−*28*). Three possible reasons are considered for this low intensity. (1) Weak resonance interaction between the two Chl molecules: According to the theoretical formalism by Breton, Nabedryk, and Parson (*25, 50*), the strength of resonance interaction between the two (B)Chl molecules is one of the factors that determine the intensity of the mid-IR electronic band. Thus, weak resonance interaction between the Chl molecules in $P680^+$ can cause the low intensity. In this regard, much weaker excitonic coupling in the Qy state has been observed in P680 compared with that in P870 of purple bacteria (*7*−*11*). (2) Asymmetric structure of $P680^+$: Breton et al. (*25*) also suggested that a larger energy difference between the two eigenstates of localized charge ($P_L^+P_M$ and $P_LP_M^+$) gives lower intensity of the mid-IR band. If the dimeric structure is more asymmetric and thus the energy gap is larger in $P680^+$ than in bacterial P^+, then the intensity of the mid-IR electronic band can be lower. This view is in agreement with the ENDOR result, which showed more localized charge distribution in $P680^+$ (82:18) (*32*) than $P870^+$ in purple bacteria [e.g., 68:32 in *Rb. sphaeroides* (*70*)]. (3) Difference in Chl species: Chl*a* is the constituent of P680 while bacterial P consists of BChl*a*, -*b*, or -*g*. In fact, $P798^+$ (BChl*g* dimer) of heliobacteria showed a much smaller mid-IR electronic band than $P840^+$ (BChl*a* dimer) of green sulfur bacteria (*26, 27*), although the RC proteins of these bacteria are thought to have a close structure (*71*). Also, in $P700^+$ (Chl*a* dimer) of PS I, which has an FeS-type RC similar to the RCs of green sulfur bacteria and heliobacteria, this type of electronic band has not been observed (*27*) (although this absence of the mid-IR electronic band was explained as due to charge localization on one Chl in $P700^+$). Thus, it is possible that Chl*a*, which has a macrocycle structure different from BChl, originally gives a weaker mid-IR electronic band.

Another prominent feature in the $P680^+/P680$ spectrum was the strong intensity of the 1179 cm^{-1} band of P680 (Figure 4b). This band may correspond to the macrocycle vibrational mode at 1188 cm^{-1} calculated by Boldt et al. (*47*) for nickel(II) methylmesopyropheophorbide *a* (NiMPPh) and nickel(II) methylpyropheophorbide *a* (NiPPh), which have the same chlorin ring as Chl*a*. According to their calculation, this mode is mainly contributed by in-plain deformation of rings IV and V. Thus, it is possible that the pronounced intensity of the 1179 cm^{-1} band is attributed to the distortion of these rings, which could be brought about by interactions of C═O groups on ring V with surrounding proteins. Such distortion of the macrocycle could be related to the extremely high redox potential of P680.

Structural Model of the Chl Molecules Coupled in the Cation, Triplet, and Qy Singlet States. So far, various structural models of P680 have been proposed [reviewed in ref (*2, 16*)] based on the following observations and ideas: (1) The basic structure and the pigment location of the PS II RC follow those of the purple bacterial RC. In particular, the His ligands of P in the bacterial L and M subunits are conserved in the D1 and D2 subunits of PS II, and hence Chl molecules corresponding to the bacterial special pair may be present in PS II. (2) Some drastic structural difference from P of purple bacteria could exist in P680, so that P680 has an extraordinary high redox potential [∼1.1 V (*4*)]. (3) Excitonic coupling in the Qy state of Chl molecules in P680 is significantly weak (*7*−*11*). (4) The spin-polarized triplet state resides on P680, because the optical bleach upon triplet formation (triplet minus singlet) is observed at ∼680 nm (*9*−*11, 72*−*74*), and thus this triplet state has been denoted as ^{3}P680. (5) The triplet state is localized on one Chl at very low temperatures but thermally equilibrates between the two Chl molecules at higher temperatures (*20, 75, 76*). (6) The *z* axis of the triplet state at helium temperature is tilted by 30° relative to the membrane normal; that is, the macrocycle of this Chl is arranged almost parallel to the membrane plane (*12*).

Difficulty in making a structural model of P680 exists in reconciling the parallel orientation of the Chl plane with the structure of the bacterial special pair, in which both of the BChl molecules are oriented perpendicular to the membrane. To overcome this problem, the following models have been proposed: (1) P680 is a monomeric Chl corresponding to the accessory BChl, which is oriented nearly parallel to the membrane (*12*). (2) P680 is a dimer in which the two Chl molecules have (anti)parallel Qy transitions and both of them are oriented nearly parallel to the membrane (*17, 18*). (3)

P680 is a dimer in which one Chl is perpendicular and the other is parallel to the membrane and the triplet state is mainly located on the latter Chl at low temperatures (*12*, *20*). Although we previously favored model 3 in the FTIR study of ^{3}P680 (*20*), it has been pointed out that this model (as well as model 2) requires significant perturbation of the protein but such perturbation is difficult under the homology of the D1 and D2 subunits with the L and M subunits of purple bacterial (*12*, *19*, *74*).

The present P680$^+$/P680 spectrum (Figure 6c) in comparison with the triplet/singlet spectrum (Figure 6d), however, showed that the main bleached band of keto C_9═O at 1669 cm^{-1} upon triplet formation was in disagreement with the bleached bands at 1704 and 1679 cm^{-1} upon cation formation, indicating that the Chl molecule, on which the triplet is mainly located at low temperatures, is not a constituent of P680. Thus, we are released from the above difficulty in making a P680 model including a parallel Chl orientation. The Qy bleach at ~680 nm upon triplet formation can be rationalized by a recent consensus that there is another Chl molecule (or excitonically coupled state consisting of several Chls) that has an absorption peak at 680−684 nm besides P680 (*10*, *39*, *40*, *77*−*83*). This bleach can also be explained by the multimer model of P680 (*21*); i.e., if the 680 nm peak originates from relatively weak excitonic coupling among several Chl and Pheo molecules including the primary donor and the triplet-possessing Chl, the triplet formation will bleach this 680 nm peak.

In Figure 7 are presented the structural models of Chl molecules coupled in the cation, triplet, and Qy singlet states. To avoid confusion, the term 'P680' is confined to the Chl molecules as the primary donor, which is equivalent to the special pair in bacterial RC. Also, we newly designate the Chl molecule that mainly possesses a triplet state at low temperatures as Chl$_T$. From the observation of a mid-IR electronic band of P680$^+$ analogous to the band of bacterial P$^+$, we consider that the structure of the bacterial special pair is basically conserved in P680 and the positive charge is delocalized over this dimer. We do not need to change the angle of macrocycle any more, and thus it remains perpendicular to the membrane. However, to realize the weaker excitonic coupling between the Chl molecules, the distance between the two Chl molecules may be longer than that of bacterial P as suggested previously (*8*, *11*, *17*, *19*). Chl$_T$ corresponds to the accessory BChl in bacterial RC and has a parallel orientation. The triplet state produced by charge recombination mostly migrates to Chl$_T$ at low temperatures. This idea of triplet migration has been originally proposed by Rutherford (*84*), but experimental support has not been obtained so far. At higher temperatures, the triplet state on Chl$_T$ equilibrates with ^{3}P680 (either or both of the Chl molecules in the special pair), although in the previous studies this equilibration has been attributed to the two Chl molecules in ^{3}P680 (*20*, *75*, *76*). The energy gap between the equilibrating triplet states has been reported as 8.4 meV by our previous FTIR study (*20*) and as 12−13 meV by EPR measurements (*75*, *76*) and now this gap is interpreted as the energy difference between ^{3}Chl$_T$ and ^{3}P680.

Model I in Figure 7 is the case that P680 and Chl$_T$ have basically independent Qy bands, both of which have peaks around 680 nm. Model II is in the context of the multimer model (*21*); P680 and Chl$_T$ are excitonically coupled and

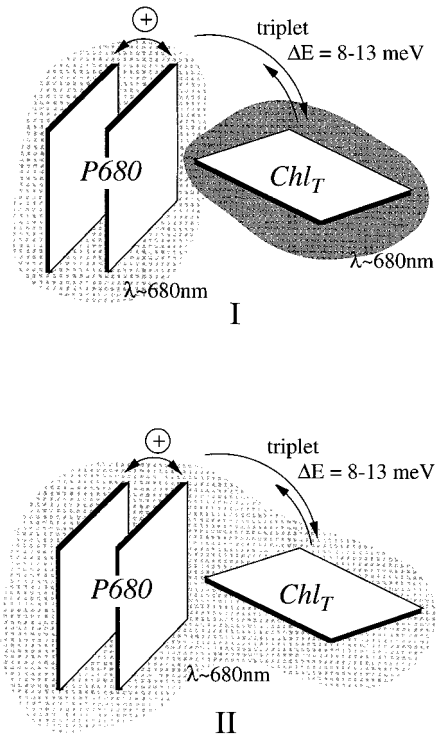

FIGURE 7: Structural models of the Chl molecules coupled in the cation, triplet, and Qy singlet states. The term 'P680' is confined to the Chl molecules that possess a positive charge as the primary donor. Chl$_T$ is a Chl on which the triplet state mainly resides at low temperatures. In this model, positions and orientations of the Chl molecules basically follow those of the BChl molecules in the RC of purple bacteria. P680 is equivalent to the bacterial special pair that is oriented perpendicular to the membrane plane, and in P680$^+$, the hole is delocalized over (or hopping between) the two Chl constituents. Chl$_T$ corresponds to the accessory BChl$_L$ or BChl$_M$ that has nearly parallel orientation, and the triplet state equilibrates with P680 with an energy gap of 8−13 meV (*20*, *75*, *76*). In model I, P680 and Chl$_T$ have basically independent Qy transitions but exhibit bands at an almost identical position of ~680 nm. Model II is in the context of the excitonic multimer (*21*), in which Chls including P680 and Chl$_T$ have an excitonically coupled Qy band at ~680 nm.

produce a Qy band at 680 nm. This excitonic multimer might include other Chl or Pheo molecules. It should be noted that Kwa et al. (*9*) proposed a model similar to model II: P680 is an $N = 3$ multimer consisting of structural equivalents of BChl$_L$ (on which the triplet is localized), P$_M$, and BPheo$_L$ (P$_L$ is missing in this model).

The keto C_9═O bands of P680 were observed at 1704 and/or 1679 cm^{-1} (Figure 6c). Recently, Hienerwadel et al. (*85*) suggested the possiblility that the differential signal at 1697(+)/1704(−) cm^{-1} (+ and − indicate positive and negative intensities, respectively) in the $Y_D^{\bullet}/Y_D$ FTIR spectrum arises from an electrochromic shift of the keto C_9═O of P680. Zhang et al. (*69*) also found a similar differential signal at 1699(+)/1707(−) cm^{-1} in their $Y_Z^{\bullet}Q_A^-/Y_ZQ_A$ spectrum. In fact, according to the computer modeling of PS II RC based on the X-ray structure of bacterial RC (*19*), the keto C_9═O bonds of P_1 and P_2 (P_1 and P_2 indicate the Chl molecules constituting P680 on the D1 and D2 subunits, respectively) point to Y_Z and Y_D, respectively, at a distance of <10 Å. The direction of the shift, i.e., the downshift when the positive charge is on (or near) Y_Z or Y_D, is also reasonable. If the above differential signals are really from the keto C_9═O bands of P680, then this will indicate that

the negative band at 1704 cm^{-1} in the $P680^+/P680$ spectrum (Figure 6c) includes both keto C_9═O vibrations of P680, which are free from hydrogen-bonding interaction. To reach a final conclusion, however, further work using site-directed mutagenesis will be necessary.

Because the His residues that ligate the accessory BChl molecules in purple bacterial RC are not conserved in the D1 and D2 subunits, there is no evidence that Chl molecules are present at the same positions. However, Chl_T has almost the same orientation as the accessory BChl with regard to the plane angle (30°) relative to the membrane (*12*). Although van Mieghem et al. (*12*) first proposed that the Chl plane is rotated by 45° relative to the accessory BChl, recalculation by Kwa et al. (*9*) provided the possibility that equivalence between the orientation of accessory BChl and Chl_T was almost exact. As suggested by Svensson et al. (*19*), the ligands of these Chl molecules can be polar groups other than histidine or water. The X-ray crystal structure of *Rps. viridis* RC showed that the keto C_9═O group of both accessory BChls is hydrogen-bonded to a water molecule that has additional hydrogen bonds to the His ligand of P and the backbone amide. The FTIR result that the keto C_9═O of Chl_T is hydrogen-bonded (*20*) suggests that a similar hydrogen-bonding network might exist around Chl_T. We cannot decide which subunit, D1 or D2, the Chl_T is attached to at the present stage. The D2 subunit might be favored in analogy with triplet migration to a carotenoid on the M subunit through $BChl_M$ in bacterial RC, while the D1 subunit might be favored when one considers that photodegradation of the D1 subunit occurs most likely through the triplet state (*86*). The possibility that Chl_T is identical to Chl_Z is excluded from the difference in the keto C_9═O positions [1669 cm^{-1} in Chl_T (Figure 6d) (*20*) and 1684 cm^{-1} in Chl_Z (Figure 4d) (*36*)].

If the Chl molecules keep the basic positions and orientations in PS II RC compared with the bacterial ones as shown in Figure 7, the reason for the extremely high redox potential of P680 (~1.1 V) cannot be found in the drastic change in the coupling between the Chl molecules in P680. Although weakened coupling by a longer Chl−Chl distance in P680 will increase the potential, still it would be lower than the monomeric Chl in vitro [~0.8 V (*6*)]. As suggested above, distortion of the macrocycle might contribute to the increase in the redox potential, but we do not know how much effect is expected. Thus, the environmental effect by the surrounding proteins should play an important role in increasing the potential. It is possible that the similar environmental factors are effective to Chl_T to increase its redox potential even higher than that of P680 so that oxidation of Chl_T by P680 is prevented.

REFERENCES

1. Michel, H., and Deisenhofer, J. (1988) *Biochemistry 27*, 1−7.
2. Diner, B. A., and Babcock, G. T. (1996) in *Oxygenic Photosynthesis: The Light Reactions* (Ort, D. R., and Yocum, C. F., Eds.) pp 213−247, Kluwer, Dordrecht.
3. Britt, R. D. (1996) in *Oxygenic Photosynthesis: The Light Reactions* (Ort, D. R., and Yocum, C. F., Eds.) pp 137−164, Kluwer, Dordrecht.
4. Klimov, V. V., Allakhverdiev, S. I., Demeter, S., and Krasnovskii, A. A. (1979) *Dokl. Akad. Nauk. SSSR 249*, 227−230.
5. Lin, X., Murchison, H. A., Nagarajan, V., Parson, W. W., Allen, J. P., and Williams, J. C. (1994) *Proc. Natl. Acad. Sci. U.S.A. 91*, 10265−10269.
6. Watanabe, T., and Kobayshi, M. (1991) in *Chlorophylls* (Scheer, H., Ed.) pp 287−315, CRC Press, Boca Raton.
7. Tetenkin, V. L., Gulyaev, B. A., Seibert, M., and Rubin, A. B. (1989) *FEBS Lett. 250*, 459−463.
8. Braun, P., Greenberg, B. M., and Scherz, A. (1990) *Biochemistry 29*, 10376−10387.
9. Kwa, S. L. S., Eijckelhoff, C., van Grondelle, R., and Dekker, J. P. (1994) *J. Phys. Chem. 98*, 7702−7711.
10. Chang, H.-C., Jankowiak, R., Reddy, N. R. S., Yocum, C. F., Picorel, R., Seibert, M., and Small, G. J. (1994) *J. Phys. Chem. 98*, 7725−7735.
11. Carbonera, D., Giacometti, G., and Agostini, G. (1994) *FEBS Lett. 343*, 200−204.
12. Van Mieghem, F. J. E., Satoh, K., and Rutherford, A. W. (1991) *Biochim. Biophys. Acta 1058*, 379−385.
13. Deisenhofer, J., Epp, O., Miki, K., Huber, R., and Michel, H. (1985) *Nature 318*, 618−624.
14. Allen, J. P., Feher, G., Yeates, T. O., Komiya, H., and Rees, D. C. (1987) *Proc. Natl. Acad. Sci. U.S.A. 84*, 5730−5734.
15. El-Kabbani, O., Chang, C.-H., Tiede, D., Norris, J., and Schiffer, M. (1991) *Biochemistry 30*, 5361−5369.
16. Satoh, K. (1996) in *Oxygenic Photosynthesis: The Light Reactions* (Ort, D. R., and Yocum, C. F., Eds.) pp 193−211, Kluwer, Dordrecht.
17. Bosch, M. K., Proskuryakov, I. I., Gast, P., and Hoff, A. J. (1995) *J. Phys. Chem. 99*, 15310−15316.
18. Schelvis, J. P. M., van Noort, P. I., Aartsma, T. J., and van Gorkom, H. J. (1994) *Biochim. Biophys. Acta 1184*, 242−250.
19. Svensson, B., Etchebest, C., Tuffery, P., van Kan, P., Smith, J., and Styring, S. (1996) *Biochemistry 35*, 14486−14502.
20. Noguchi, T., Inoue, Y., and Satoh, K. (1993) *Biochemistry 32*, 7186−7195.
21. Durrant, J. R., Klug, D. R., Kwa, S. L. S., van Grondelle, R., Porter, G., and Dekker, J. P. (1995) *Proc. Natl. Acad. Sci. U.S.A. 92*, 4798−4802.
22. Mäntele, W. G. (1995) in *Anoxygenic Photosynthetic Bacteria* (Blankenship, R. E., Madigan, M. T., and Bauer, C. E., Eds.) pp 627−647, Kluwer, Dordrecht.
23. Nabedryk, E. (1996) in *Infrared Spectroscopy of Biomolecules* (Mantsch, H. H., and Chapman, D., Eds.) pp 39−81, Wiley-Liss, New York.
24. Mäntele, W., Nabedryk, E., Tavitian, B. A., Kreutz, W., and Breton, J. (1985) *FEBS Lett. 187*, 227−232.
25. Breton, J., Nabedryk, E., and Parson, W. W. (1992) *Biochemistry 31*, 7503−7510.
26. Noguchi, T., Kusumoto, N., Inoue, Y., and Sakurai, H. (1996) *Biochemistry 35*, 15428−15435.
27. Nabedryk, E., Leibl, W., and Breton, J. (1996) *Photosynth. Res. 48*, 301−308.
28. Noguchi, T., Fukami, Y., Oh-oka, H., and Inoue, Y. (1997) *Biochemistry 36*, 12329−12336.
29. Nabedryk, E., Leonhard, M., Mäntele, W., and Breton, J. (1990) *Biochemistry 29*, 3242−3247.
30. Nugent, J. H. A., Telfer, A., Demetriou, C., and Barber, J. (1989) *FEBS Lett. 255*, 53−58.
31. Telfer, A., and Barber, J. (1989) *FEBS Lett. 246*, 223−228.
32. Rigby, S. E. J., Nugent, J. H. A., and O'Malley, P. J. (1994) *Biochemistry 33*, 10043−10050.
33. Tomo, T., and Satoh, K. (1994) *FEBS Lett. 351*, 27−30.
34. Berthold, D. A., Babcock, G. T., and Yocum, C. F. (1981) *FEBS Lett. 134*, 231−234.
35. Ono, T., and Inoue, Y. (1986) *Biochim. Biophys. Acta 850*, 380−389.
36. Noguchi, T., and Inoue, Y. (1995) *FEBS Lett. 370*, 241−244.
37. Noguchi, T., Mitsuka, T., and Inoue, Y. (1994) *FEBS Lett. 356*, 179−182.
38. Van Kan, P. J. M., Otte, S. C. M., Kleinherenbrink, F. A. M., Nieveen, M. C., Aartsma, T. J., and van Gorkom, H. J. (1990) *Biochim. Biophys. Acta 1020*, 146−152.

39. Cattaneo, R., Zucchelli, G., Garlaschi, F. M., Finzi, L., and Jennings, R. C. (1995) *Biochemistry 34*, 15267−15275.
40. Konermann, L., and Holzwarth, A. R. (1996) *Biochemistry 35*, 829−842.
41. Schenck, C. C., Diner, B., Mathis, P., and Satoh, K. (1982) *Biochim. Biophys. Acta 680*, 216−227.
42. Van Dorssen, R. J., Breton, J., Plijter, J. J., Satoh, K., van Gorkom, H. J., and Amesz, J. (1987) *Biochim. Biophys. Acta 893*, 267−274.
43. Tomo, T., Mimuro, M., Iwaki, M., Kobayashi, K., Itoh, S., and Satoh, K. (1997) *Biochim. Biophys. Acta 1321*, 21−30.
44. Takahashi, Y., Hansson, Ö., Mathis, P., and Satoh, K. (1987) *Biochim. Biophys. Acta 893*, 49−59.
45. Fujiwara, M., and Tasumi, M. (1986) *J. Phys. Chem. 90*, 250−255.
46. Fujiwara, M., and Tasumi, M. (1986) *J. Phys. Chem. 90*, 5646−5650.
47. Boldt, N. J., Donohoe, R. J., Birge, R. R., and Bocian, D. F. (1987) *J. Am. Chem. Soc. 109*, 2284−2298.
48. Tasumi, M., and Fujiwara, M. (1987) in *Spectroscopy of Inorganic-Based Materials* (Clark, R. J. H., and Hester, R. E., Eds.) pp 407−428, John Wiley & Sons, Chichester.
49. Breton, J., Hienerwadel, R., and Nabedryk, E. (1997) in *Spectroscopy of Biological Molecules: Modern Trends* (Carmona, P., Navarro, R., and Hernanz, A., Eds.) pp 101−102, Kluwer, Dordrecht.
50. Parson, W. W., Nabedryk, E., and Breton, J. (1992) in *The Photosynthetic Bacterial Reaction Center II* (Breton, J., and Verméglio, A., Eds.) pp 79−88, Plenum Press, New York.
51. Gasyna, Z., and Schatz, P. N. (1996) *J. Phys. Chem. 100*, 1445−1448.
52. Reimers, J. R., and Hush, N. S. (1995) *Chem. Phys. 197*, 323−332.
53. Koulougliotis, D., Innes, J. B., and Brudvig, G. W. (1994) *Biochemistry 33*, 11814−11822.
54. Janoschek, R., Weidemann, E. G., and Zundel, G. (1973) *J. Chem. Soc., Faraday Trans. 2 69*, 505−520.
55. Zundel, G. (1988) *J. Mol. Struct. 177*, 43−68.
56. Moënne-Loccoz, P., Robert, B., and Lutz, M. (1989) *Biochemistry 28*, 3641−3645.
57. Krawczyk, S. (1989) *Biochim. Biophys. Acta 976*, 140−149.
58. Koyama, Y., Umemoto, Y., and Akamatsu, A. (1986) *J. Mol. Struct. 146*, 273−287.
59. Bekárek, V., Kaplanová, M., and Socha, J. (1979) *Stud. Biophys. 77*, 21−24.
60. Surewicz, W. K., and Mantsch, H. H. (1988) *Biochim. Biophys. Acta 952*, 115−130.
61. Allakhverdiev, S. I., Ahmed, A., Tajmir-Riahi, H.-A., Klimov, V. V., and Carpentier, R. (1994) *FEBS Lett. 339*, 151−154.
62. Berthomieu, C., Nabedryk, E., Mäntele, W., and Breton, J. (1990) *FEBS Lett. 269*, 363−367.
63. Berthomieu, C., Boussac, A., Mäntele, W., Breton, J., and Nabedryk, E. (1992) *Biochemistry 31*, 11460−11471.
64. Hienerwadel, R., and Berthomieu, C. (1995) *Biochemistry 34*, 16288−16297.
65. Hienerwadel, R., Boussac, A., Breton, J., and Berthomieu, C. (1996) *Biochemistry 35*, 15447−15460.
66. Noguchi, T., Ono, T., and Inoue, Y. (1992) *Biochemistry 31*, 5953−5956.
67. Noguchi, T., Ono, T., and Inoue, Y. (1995) *Biochim. Biophys. Acta 1228*, 189−200.
68. Noguchi, T., and Inoue, Y. (1995) *J. Biochem. 118*, 9−12.
69. Zhang, H., Razeghifard, M. R., Fischer, G., and Wydrzynski, T. (1997) *Biochemistry 36*, 11762−11768.
70. Rutter, J., Lendzian, F., Schulz, C., Fetsch, A., Kuhn, M., Lin, X., Williams, J. C., Allen, J. P., and Lubitz, W. (1995) *Biochemistry 34*, 8130−8143.
71. Liebl, U., Mockensturm-Wilson, M., Trost, J. T., Brune, D. C., Blankenship, R. E., and Vermaas, W. (1993) *Proc. Natl. Acad. Sci. U.S.A. 90*, 7124−7128.
72. Den Blanken, H. J., Hoff, A. J., Jongenelis, A. P. J. M., and Diner, B. A. (1983) *FEBS Lett. 157*, 21−27.
73. Van der Vos, R., van Leeuwen, P. J., Braun, P., and Hoff, A. J. (1992) *Biochim. Biophys. Acta 1140*, 184−198.
74. Hillmann, B., Brettel, K., van Mieghem, F., Kamlowski, A., Rutherford, A. W., and Schlodder, E. (1995) *Biochemistry 34*, 4814−4827.
75. Kamlowski, A., Frankemöller, L., van der Est, A., Stehlik, D., and Holzwarth, A. R. (1996) *Ber. Bunsen-Ges. Phys. Chem. 100*, 2045−2051.
76. Bosch, M. K., Proskuryakov, I. I., Gast, P., and Hoff, A. J. (1996) *J. Phys. Chem. 100*, 2384−2390.
77. Konermann, L., Yruela, I., and Holzwarth, A. R. (1997) *Biochemistry 36*, 7498−7502.
78. Merry, S. A. P., Kumazaki, S., Tachibana, Y., Joseph, D. M., Porter, G., Yoshihara, K., Barber, J., Durrant, J. R., and Klug, D. R. (1996) *J. Phys. Chem. 100*, 10469−10478.
79. Groot, M.-L., Dekker, J. P., van Grondelle, R., den Hartog, F. T. H., and Völker, S. (1996) *J. Phys. Chem. 100*, 11488−11495.
80. Groot, M.-L., van Mourik, F., Eijckelhoff, C., van Stokkum, I. H. M., Dekker, J. P., and van Grondelle, R. (1997) *Proc. Natl. Acad. Sci. U.S.A. 94*, 4389−4394.
81. Kwa, S. L. S., Tilly, N. T., Eijckelhoff, C., van Grondelle, R., and Dekker, J. P. (1994) *J. Phys. Chem. 98*, 7712−7716.
82. Chang, H.-C., Small, G. J., and Jankowial, R. (1995) *Chem. Phys. 194*, 323−333.
83. Eijckelhoff, C., Vacha, F., van Grondelle, R., Dekker, J. P., and Barber, J. (1997) *Biochim., Biophys. Acta 1318*, 266−274.
84. Ratherford, A. W. (1986) *Biochem. Soc. Trans. 14*, 15−17.
85. Hienerwadel, R., Boussac, A., Breton, J., Diner, B. A., and Berthomieu, C. (1997) *Biochemistry 36*, 14712−14723.
86. Vass, I., Styring, S., Hundal, T., Koivuniemi, A., Aro, E.-M., and Andersson, B. (1992) *Proc. Natl. Acad. Sci. U.S.A. 89*, 1408−1412.

BI9812975